also are able to display transitions not only from disorder to order (synergetic behavior) but also from order to complexity (temporal and spatio-temporal instabilities and chaos).

This revolution entered the field of optics[2] around 1975 with Haken's discovery[3] of the isomorphism between the three Lorenz equations[1,4] and the single mode homogeneously broadened laser equations. Unfortunately, the experimental realization of a chaotic Lorenz-Haken laser has proven a challenging problem, in spite of the fact that, since the beginning of experimental studies in lasers, they have shown irregular dynamical pulsations. Only recently, a coherently pumped far-infrared ammonia laser has allowed the first observation of a behavior remarkably similar with the predictions of the paradigmatic Lorenz-Haken model.[5,6]

However, the theoretical understanding of the dynamics of this ammonia laser on the basis of the Lorenz-Haken theory, has raised considerable controversy [5,7,8] for the inability of this model to describe important physical aspects of the real system. Thus, while two-level (i.e., incoherently pumped) lasers are considered in the Lorenz-Haken model, coherently pumped lasers operate on a three-level scheme. In such conditions, the coherent pump laser field not only affects the populations of various energy levels, but can also induce a strong interaction with the generated field through nonlinear coherent effects such as the Ramon process and the AC Stark effect. This can result in new dynamic features of the coherently pumped lasers.[2b,7,9]

Indeed, the numerical study[10] of a homogeneously-broadened three-level laser model—for a parameter range appropriate for the ammonia laser—revealed striking differences between the theoretical predictions and the experimental observations[5] of Lorenz-like behavior in this laser.

By our incorporating the Doppler-broadening in the three-level laser model, considering operation in the backward emission direction, as in the experiments[5], and analyzing the dynamics of the laser phase in addition to that of intensity, we have been able to reproduce[8,11] qualitatively the main experimental features of the heteroclynic or Lorenz-type behavior observed in the experiments[5], including instability pump threshold, detuning-pump bifurcation diagram, and symmetric spiral attractor. The incorporation of the Doppler broadening complicates considerably the laser model, which in our case was composed by 217 coupled ordinary differential equations. It is remarkable that such a complex model predicts a behavior so similar to that of the simple three (or five for the detuned laser) equations model for the Lorenz-Haken laser.

Coherently pumped lasers have thus become most interesting systems for nonlinear dynamics with the first demonstration of Lorenz-like dynamics in the real world. Moreover, these lasers are very versatile systems that include as limit simple cases the two-level laser (when coherent pumping effects are eliminated) and the Raman laser (when the detunings of the pump and generated fields are equal and much larger than the molecular transitions linewidths). We believe they have also produced evidence of two rather general aspects: (1) that highly-dimensional dynamical systems can approach asymptotically in time-low dimensional attractors, and (2) that the dynamical behavior of lasers usually proves resistant to a qualitative understanding on the basis of simple models that, instead, yield a satisfactory explanation of the stable output emission.

REFERENCES

1. E.N. Lorenz, J. Atmos. Sci. 20, p. 130, 1963.
2. See for example, a) the Special Issues, J. Opt. Soc. Am. B, 2, pp. 1–272, 1985; 5, pp. 875-1211, 1988; b) C.O. Weiss and R. Vilaseca, "Laser Dynamics", Physic Verlag, Weinheim (to appear); c) "Coherence and Quantum Optics 6", J.H. Eberly, L. Mandel and E. Wolf, eds., Plenum, New York (to appear).
3. H. Haken, Phys. Lett. A 53, p. 77, 1975.
4. C. Sparrow, The Lorenz equations: Bifurcations, chaos, and strange attractors, Springer-Verlag, Berlin, 1982.
5. C.O. Weiss, N.B. Abraham, and U. Hubbner, Phys. Rev. Lett. 61. p. 1587, 1988.
6. H. Zeghlache, P. Mandel, N.B. Abraham, and C.O. Weiss, Phys. Rev. A. 38, p. 3128, 1988.
7. J.V. Moloney, W. Forysiak, J.S. Uppal, and R.G. Harrison, Phys. Rev. A. 39, p. 1277, 1989 (and references therein).
8. R.Corbalan, F. Laguarta, J. Pujol, and R. Vilaseca, Opt. Commun., 71, p. 290, 1989.
9. R.G. Harrison, W. Lu, and P.K. Gupta, Origin of pulsating instabilities and chaos in Raman lasers, in ref. 2 c); Phys. Rev. Lett. 63, p. 1372.
10. J. Pujol, F. Laguarta, R. Vilaseca, and R. Corbalan, J. Opt. Soc. Am. B, 5, p. 1004, 1988.
11. E. Roldan, G.J. de Valcarcel, R. Vilaseca, F. Silva, J. Pujol, R. Corbalan, and F. Laguarta, Phase dynamics in a Doppler-broadened optically-pumped laser, Opt. Commun. (submitted July 1989).

Second harmonic generation in periodically-poled $LiNbO_3$

G.A. Magel, E.J. Lim, M.M. Fejer, and R.L. Byer,
Stanford University

Compact, solid-state sources of coherent blue light have applications in biomedicine, displays, printing, and optical storage. Because blue semiconductor diode lasers are not currently available, techniques for the efficient nonlinear optical frequency conversion of infrared diode

lasers are being developed. Materials with high nonlinearity and good optical quality are therefore in demand. Engineering the optical properties of a well-studied material such as lithium niobate ($LiNbO_3$) provides an alternative to the search for entirely new materials. Using quasi-phase-matching in $LiNbO_3$, we have accomplished collinear cw second harmonic generation (SHG) with wavelengths and nonlinear coefficients that have been impossible to phase-match using only the material birefringence.

Quasi-phase-matching (QPM) was the first technique to be suggested for compensating refractive-index dispersion to obtain efficient SHG.[1] By periodically reversing the sign of the nonlinear coefficient at odd integer multiples of the coherence length, continuous power flow from the fundamental into the second harmonic wave can be maintained along the interaction length. While the highest conversion efficiency is obtained when reversals occur every coherence length, fabrication considerations may compel the use of longer distances between reversals. In $LiNbO_3$, the signs of the nonlinear coefficients are tied to the orientation of ferroelectric domains, and thus QPM can be accomplished in a crystal with a periodically-alternating domain structure (periodically-poled $LiNbO_3$). We have developed two methods to produce periodically-poled $LiNbO_3$ for QPM nonlinear optical interactions.

We have produced periodically-poled $LiNbO_3$ crystals up to 0.5 mm in diameter using laser-heated pedestal growth.[2] In this technique, the output of a CO_2 laser is focused on the tip of a typically 500-μm diameter source rod of $LiNbO_3$ to make a small molten droplet into which a seed crystal is dipped. The seed is then withdrawn from the droplet as fresh source material is supplied. Periodically-reversed ferroelectric domains can be created during growth either by rotating an asymmetric heat input or by periodically modulating the heating power. Using these techniques, we have grown domain structures with periods as small as 2 μm in either nominally 5% Mg-doped or undoped congruent material and in crystals grown along either the x or z axis.

Previous demonstrations of quasi-phase-matched SHG in $LiNbO_3$ have used Czochralski-grown crystals with poling periods down to 6.8 μm for frequency doubling 1.06 μm light.[3] The shorter periods attainable using pedestal growth have allowed us to apply this material to room temperature, quasi-phase-matched SHG of light at wavelengths as short as 407 nm, using the d_{33} and d_{22} nonlinear coefficients. The theoretical conversion efficiency using d_{33} and QPM with domain lengths equal to the coherence length is ≈13.5 times that which would be obtained were it possible to birefringently phase-match an interaction at this wavelength with the commonly used d_{31} coefficient. The conversion efficiencies and wavelength and temperature tuning bandwidths we have measured are consistent with an effective interaction length of ≈320 μm (>230 domains). No photorefractive damage was observed at the relatively low levels of blue light generated in the SHG experiments, and a separate test with cw focused 488 nm beams showed that the periodically-poled material exhibits no discernible photorefractivity at intensities up to 200 kW/cm.[2]

Waveguides increase the efficiency of nonlinear optical interactions by maintaining high optical intensities over considerable lengths. We have developed a method to produce periodically-poled $LiNbO_3$ waveguides in standard integrated-optic substrates, using commonly used materials and process. It is known that the diffusion of titanium into the +z face of a $LiNbO_3$ wafer causes ferroelectric domain reversal at the surface of the wafer. By indiffusing lithographically-defined gratings of titanium, we exploit this effect to produce periodic arrays of alternating domains. Waveguides are then made in the periodically-poled surface using the annealed-proton-exchange technique.

In waveguide doublers poled with periods on the order of 7 μm, about 1 μW of blue light at 410 nm has been generated using the d_{33} coefficient in a 1 mm-long grating with a normalized conversion efficiency of about 40%/W-cm^2.[4] The observed wavelength tuning bandwidth is consistent with an effective length approximately equal to the grating length. The measured conversion efficiency implies that in cm-long devices, mW levels of blue light could be produced from tens of mW of infrared fundamental power. Work is underway to demonstrate this scaling with length and also to further improve the efficiency by making the domains one coherence length long instead of three. In addition to the work on blue light generation, SHG of green light has been observed in devices fabricated using Ti gratings with larger periods.[5] Other workers have demonstrated SHG in periodically-poled $LiNbO_3$ waveguides produced with a different process.[6]

REFERENCES

1. J.A. Armstrong, N.Bloembergen, J. Ducuing, and P.S. Pershan, Phys. Rev. 127, p. 1918, 1962.
2. G.A. Magel, M.M. Fejer, and R.L. Byer, to be published in Appl. Phys. Lett.; M.M. Fejer, J.L. Nightingale, G.A. Magel, and R.L. Byer, Rev. Sci. Instrum. 55, p. 1791, 1984.
3. Y.H. Xue, N.B. Ming, J.S. Zhu, and D. Feng, Chinese Phys. 4, p. 554, 1983; A. Feisst and P. Koidl, Appl. Phys. Lett. 47, p. 1125, 1985.
4. E.J. Lim, M.M. Fejer, R.L. Byer, and W.J. Kozlovsky, Electron. Lett. 25, p. 731, 1989.
5. E.J. Lim, M.M. Fejer, and R.L. Byer, Electron. Lett. 25, p. 174, 198
6. J. Webjorn, F. Laurell, and G. Arvidsson, Phot. Tech. Lett., 1, 31 1989.

Quasi-phase-matched interactions in lithium niobate

M. M. Fejer, G. A. Magel, and E. J. Lim

Edward L. Ginzton Laboratory
Stanford University, Stanford, California 94305

ABSTRACT

Phase-matching nonlinear interactions by periodic variations in the nonlinear susceptibility, quasi-phase-matching, offers advantages in accessible tuning range and in choice of nonlinear coefficients over the conventional birefringent technique. Periodically reversed ferroelectric domains can be used to create monolithic structures with the necessary high-spatial-frequency variations in the nonlinear susceptibility. We present two techniques for the fabrication of periodically-poled lithium niobate crystals, and results for bulk and guided-wave second harmonic generation of blue and green light.

1. INTRODUCTION

Recent advances in III-V diode laser technology have led to the commercial availability of near-infrared diode lasers with single mode output powers in excess of 100 mW. The more difficult materials problems involved in producing similar diode lasers for the visible or the mid-infrared have not yet been solved. Thus, nonlinear optical devices suitable for frequency conversion of existing diode-laser pump sources are of considerable technological interest. Because single-pass bulk nonlinear devices cannot operate efficiently at the pump powers available with diode lasers, resonant enhancement of the fundamental fields,[1,2] or waveguide confinement[3,4] is necessary for the generation of useful amounts of output radiation. Materials used in these devices must meet stringent requirements on their nonlinear susceptibility, transparency, and particularly on their birefringence for phase-matching. Lithium niobate, which has large nonlinear susceptibilities, transparency from 350 nm – 4000 nm, well-developed waveguide technologies, and ready commercial availability, is an attractive material for these applications. Unfortunately, the usefulness of lithium niobate is limited by its birefringence, which is too small for second harmonic generation (SHG) of blue light and too large for noncritical phase-matching of difference frequency generation of mid-infrared radiation. We describe here the use of periodic poling to achieve quasi-phase-matching, extending the applicability of lithium niobate to any interaction within its transparency range.

2. QUASI-PHASE-MATCHING

Phase-matching, broadly defined as a means for maintaining the phase relationship between the waves participating in a nonlinear interaction, is essential for efficient frequency-conversion devices. Conventionally, the phase velocity mismatch caused by dispersion of the refractive indices is compensated by use of a birefringent crystal to match the velocity of orthogonally-polarized waves. While birefringent phase-matching has been used in essentially all practical nonlinear devices, it limits the choice of nonlinear crystals to those having appropriate relationships between dispersion and birefringence, and forces the use of only those elements of the nonlinear susceptibility tensor that couple orthogonally polarized waves. Alternative approaches to phase-matching, such as modal dispersion[3] or the Cerenkov effect[4] in waveguides, are generally accompanied by reduced conversion efficiency and nonoptimal output spatial modes.

Another approach, quasi-phase-matching (QPM), was proposed early in the development of nonlinear optics.[5,6] In QPM, the interacting waves travel with different phase velocities, but accumulation of phase mismatch is prevented through appropriate spatial modulation of the sign or magnitude of the nonlinear

susceptibility. Using second harmonic generation (SHG) as an example, the wavevector mismatch Δk is given by

$$\Delta k = k_{2\omega} - 2\,k_{\omega} \ , \tag{1}$$

where the subscripts ω and 2ω refer to the fundamental and second harmonic frequencies, respectively. QPM is achieved by introducing a component of the nonlinear susceptibility with a spatial frequency equal to Δk . In the simplest form of modulation, the sign of the nonlinear susceptibility is reversed every coherence length ($l_c \equiv \pi/\Delta k$), so that the sign of the coupling coefficient between the fundamental and the second harmonic is changed at every point where a phase shift of π accumulates between the two waves. A monotonic increase in the magnitude of the second harmonic wave then results, instead of the periodic oscillation characteristic of non-phase-matched interactions. In a more general case, the sign reversal occurs every m coherence lengths. The effective nonlinear coefficient for the quasi-phase-matched interaction, d_Q, is then related to the effective nonlinear coefficient for a conventional interaction involving the same waves, d_{eff}, by the component at spatial frequency Δk of the Fourier expansion of the square wave, i.e.

$$d_Q = \begin{cases} (2/m\pi)d_{eff} & \text{for } m \text{ odd} \\ 0 & \text{for } m \text{ even} \end{cases} \ . \tag{2}$$

Note that d_Q for mth order QPM is inversely proportional to m, so that the efficiency of nonlinear devices, proportional to $(d_Q)^2$, decreases as m^{-2}. First-order interactions are thus desirable from the standpoint of efficiency, but higher-order QPM is sometimes used for ease of fabrication. The more general case where the duty cycle is not 50% is discussed in section 3.

The advantages of QPM result from the decoupling of phase-matching from material birefringence. With QPM, one can use a material for any interaction within its transparency range, adjust for phase-matching at any convenient temperature, use any of the nonlinear coefficients (including those coupling waves of the same polarization), and carry out interactions in waveguides that support only one polarization (proton exchange in lithium niobate). In many materials, the nonlinear coefficients coupling fields of the same polarization are often larger than those coupling orthogonally-polarized fields. For lithium niobate, d_{33} = 34 pm/V,[7] so that d_Q for this polarization, 22 pm/V, is 3.7 times larger than the d_{31} coefficent used for birefringent phase-matching, and the efficiency of QPM devices is 13 times larger than that of comparable birefringently phase-matched devices.

In order to be useful for device applications, the periodicity of the domains must be accurately controlled. If the spacing of the domains deviates from the ideal structure, phase error accumulates between the interacting waves, and the efficiency is reduced. The tolerance for such errors depends on the statistical nature of the variations and the length, L, of the device. It can be shown that for small random errors, the efficiency is reduced by 50% when the rms deviation, $\delta\Lambda$, of the domain period, Λ, is[8]

$$\delta\Lambda/\Lambda = (1/\pi)\sqrt{l_c/L} \tag{3}$$

while for a fixed deviation, $\Delta\Lambda$, a 50% reduction occurs when

$$\Delta\Lambda/\Lambda = (2.78/\pi)\,l_c/L \ . \tag{4}$$

Eq. (4) states essentially that the useful length of the structure is the length over which the accumulated error in the position of the last layer is one coherence length. Note that this is a rather strict criterion, since typical coherence lengths are on the order of microns and typical devices are millimeters long.

Because typical coherence lengths for interactions involving visible light are 1–10 μm, a major difficulty in QPM is modulation of the nonlinear susceptibility on the rather short spatial scale necessary for efficient interactions. The conceptually simplest approach to creation of the sign reversal, cutting the crystal into a series of wafers one coherence length long and restacking the slices with alternating 180° rotations, is feasible only for far-infrared interactions.[9,10] This difficulty can be avoided with monolithic techniques based on the sign changes in the nonlinear susceptibility associated with rotational twinning,[11] partial orientation of polymer films,[12] or reversed ferroelectric domains.[13]

Our studies of QPM have been focused on lithium niobate, which undergoes a ferroelectric transition at a Curie temperature, T_C, of approximately 1150°C to a low temperature phase with spontaneous polarization oriented parallel to the crystallographic z-axis.[14] Antiparallel ferroelectric domains, which are related crystallographically to one another by a 180° rotation around the x-axis, can easily be induced at temperatures close to T_C, but are extremely difficult to reorient at room temperature.[14] Because the signs of all components of the nonlinear susceptibility tensor change in adjacent domains, crystals with appropriately-spaced periodic domain reversals (periodically-poled lithium niobate or PPLN) can be used to achieve QPM.

Domain reversal has been induced during Czochralski growth of bulk lithium niobate crystals by periodic perturbation of the growth conditions, either through a pulsed current passed through the crystal[15] or by rotation of the crystal in an asymmetric thermal field.[16] Reversed domains with periods as small as 6.8 μm have been created by these techniques.

We report here two methods for producing PPLN crystals, one based on indiffusion of lithographically patterned dopants on planar substrates, the other based on modulation of the heat input during laser-heated pedestal growth of small diameter crystals. Frequency conversion experiments are also described, including SHG of green and blue light in planar and channel waveguides fabricated by proton exchange in the planar substrates, and bulk SHG of blue light in the pedestal-grown crystals.

3. PLANAR DEVICES

Waveguides enhance the efficiency of nonlinear optical interactions because they maintain high optical intensities over long interaction lengths. Previous guided wave devices for frequency conversion have relied on birefringence, modal dispersion, or the Cerenkov effect for phasematching. Guided wave devices using quasi-phase-matching techniques are particularly attractive for frequency conversion applications because they combine the high efficiency resulting from waveguides with the advantages of QPM discussed previously.

It is convenient to define a normalized conversion efficiency, η_{nor}, which accounts for the effective nonlinear coefficient of the material, the overlap of the fundamental and harmonic waveguide modal fields, and the effects of quasi-phase-matching. The normalized conversion efficiency η_{nor} of a quasi-phase-matched waveguide frequency doubler is related to the absolute conversion efficiency, η, by

$$\eta = \frac{P_{2\omega}}{P_{\omega}} = \eta_{nor} P_{\omega} L^2 , \tag{5}$$

where P_{ω} and $P_{2\omega}$ are the powers of the fundamental and harmonic, respectively, and L is the length over which QPM occurs.

The ideal configuration for a waveguide device which relies on periodic sign reversals of the nonlinear susceptibility for QPM requires a sign-reversal grating with a 50% duty cycle that is constant over the depth of the waveguide. In this case, η_{nor} is given by

$$\eta_{nor} = \frac{8\pi^2 d_Q^2}{n_\omega^2 n_{2\omega} c\varepsilon_0 \lambda_\omega^2} \left| \int_{-\infty}^{+\infty} E_{2\omega}^*(y)\, E_\omega^2(y)\, dy \right|^2 \tag{6}$$

where y is the depth coordinate, E_ω and $E_{2\omega}$ are the normalized modal field distributions, and n_ω and $n_{2\omega}$ are the corresponding modal effective indices of the waveguide. We have assumed a planar waveguide for simplicity; the analysis for a channel waveguide requires an additonal integral in the width dimension. The integral in Eq. (6) reflects the confinement and overlap of the modes, and is the same as appears in the theory of conventionally phase-matched waveguide interactions.[3]

In the general nonideal case, the sign reversals of the nonlinear susceptibility can be aperiodic and can vary over the depth of the waveguide. A function $g(y,z)$, taking the values ± 1, can be used to specify the spatial variation of the nonlinear coefficient according to $d_{eff}(y,z) = |d_{eff}|g(y,z)$. As will become evident from the experimental results which follow, we are interested in the nonideal periodic structure which consists of a sign-reversal grating whose duty cycle varies over the depth of the waveguide. In this case

$$\eta_{nor} = \frac{8\pi^2 d_Q^2}{n_\omega^2 n_{2\omega} c\varepsilon_0 \lambda_\omega^2} \left| \int_{-\infty}^{+\infty} G_m(y)\, E_{2\omega}^*(y)\, E_\omega^2(y)\, dy \right|^2 \tag{7}$$

Here d_Q takes the value $2d_{eff}/m\pi$ for even as well as odd m. The new quantity $G_m(y)$ in the modal overlap integral is the m^{th} coefficient of the Fourier series representation of $g(y,z)$, normalized to $(2/m\pi)$,

$$G_m(y) = \left(\frac{m\pi}{2}\right) \frac{1}{\Lambda} \int_0^\Lambda g(y,z)\, e^{-i(2m\pi/\Lambda)\, z}\, dz \tag{8}$$

For ideal, 50% duty-cycle structures with no depth dependence, G_m becomes 1 for odd m and 0 for even m, recovering the results of Eq. (6). If the penetration depth of the domains is small compared to the depth of the waveguide, the overlap integral in Eq. (7) can be substantially smaller than that for the ideal case.

We have investigated methods for creating arrays of periodically reversed ferroelectric domains at the surface of lithium niobate wafers, in which planar or channel waveguides for quasi-phase-matched nonlinear interactions can be fabricated. The conceptually simplest approach is to use an interdigital electrode to apply a periodic electric field to a crystal heated close to its Curie temperature. The domains will then align with the applied field, and be frozen into a periodic configuration as the temperature is lowered. While this technique has been successfully applied to lithium tantalate, whose Curie temperature is $\approx 620°C$,[17] it is difficult to find suitable electrode materials for lithium niobate. At temperatures close to the Curie temperature of lithium niobate, diffusion of the electrode into the substrate is a problem, especially in the presence of a poling field, which tends to enhance the penetration through electrodiffusion.

An alternative approach was suggested by the work of Nakamura, who observed that an inverted domain appears at the +z surface of lithium niobate plates heated to temperatures close to T_C.[18] The depth of the domain reversal increased with both the soak time at a given temperature and the temperature at a given soak time. One model that explains these results, and is also consistent with domain distributions observed in single crystal fibers, is that the domains align with the temperature gradients in the surface cooled bodies under the influence of thermoelectrically generated fields.[19] The influence of the soak temperature would then be due to the reduction of the coercive field as the temperature approaches T_C, while the influence of the soak time is through increased lithium outdiffusion, which reduces T_C,[20] and hence reduces the coercive field at a given temperature. We carried out further experiments, including suppression of the counter-poling by processing the crystal in a lithium-rich atmosphere, which have tended to support this model. Note that the mechanisms leading to domain reversal in lithium niobate are complex, and other effects due to gradients in the concentration may contribute to observed behavior, as discussed in section 4 below. Details of these measurements are being prepared for publication.[21] The process for periodic poling suggested by these observations is to spatially modulate the concentration of Li by outdiffusion through a periodic mask, and to choose the thermal conditions so that the lithium-poor regions counterpole while the remainder of the crystal does not. While this poling method does not require the application of electric fields, and hence allows insulating mask materials, we again found it difficult to identify an appropriate material for the mask, i.e. one that blocks Li outdiffusion but does not indiffuse into the substrate and is readily removed after the thermal processing. Encouraging results with SiO_2 masks have recently been obtained by Webjörn *et al.*[22]

Since it is difficult to find an electrode or mask material that does not diffuse into lithium niobate at elevated temperatures, a technique based on intentional indiffusion of an innocuous dopant is attractive. We have had success with a method using indiffusion of a patterned Ti film, based on the same principle as the poling method using Li concentration variations described above. Regions doped with Ti have a lower Curie temperature than do undoped regions, so that periodic doping leads to periodic domain inversion after thermal processing. This method was suggested by the observation by Miyazawa that fabrication of Ti-indiffused waveguides on +z substrates is often accompanied by domain reversal.[23,24]

We investigated a range of Ti film thicknesses, stripe widths, soak temperatures, and soak times with the goal of reducing the Ti concentration as much as possible to minimize changes in the refractive index while maintaining well-defined regions of domain reversal with adequate penetration depth for good overlap with the waveguide modes. As the number of parameters is large, an optimum process has not yet been identified, but useful results have been obtained with 50–300 Å thick Ti films patterned with liftoff lithography, process temperatures of 1000–1100°C, and soak times less than one hour. Bearing in mind the isotropic nature of Ti diffusion,[25] the parameters should be chosen to prevent excessive overlap of the Ti distributions from adjacent lines. To prevent simultaneous lithium outdiffusion, the poling process was carried out in a closed alumina boat filled with congruent lithium niobate powder. Details of processes for specific devices are discussed later in this section. Typical results are shown in Figs. 1 and 2, which are photomicrographs of the top (z) and end (y) faces of periodically-poled wafers which have been etched for 30 minutes at room temperature in HF to reveal the domain structure. The sharply delineated domains created by this process can be seen in Fig. 1. The triangular shape of the domains in Fig. 2 is typical for cases where the depth of the reversed regions is comparable to the period of the structure. Domains shallower than the period of the structure tend to be more rectangular in cross-section. As is characteristic of diffusion driven processes, the periodic variations in the dopant concentration that cause the poling tend to wash out if the diffusion depth is larger than the period of the structure, which limits the attainable depth of domain reversal.

To fabricate a waveguide in the periodically-poled substrates, a low-temperature process is desirable to prevent erasure of the domain pattern. Proton exchange, which is typically carried out at 200–300°C, is ideal for this purpose, and has the additional advantage of reducing the photorefractive sensitivity of the waveguide. While waveguides fabricated by this process, which guide only z-polarized modes, cannot be

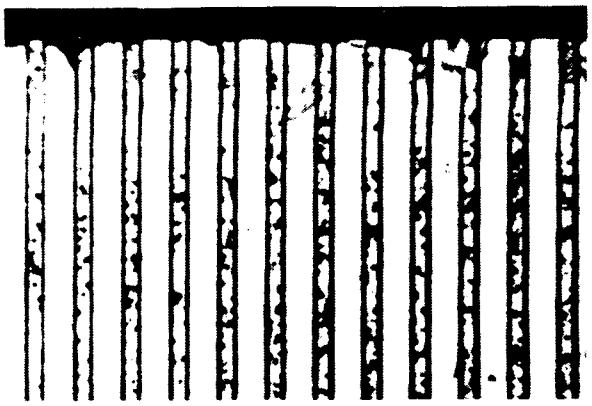

Fig.1. Periodic domains on the z-face of a lithium niobate wafer revealed by etching in HF acid. Period of pattern is 10 μm.

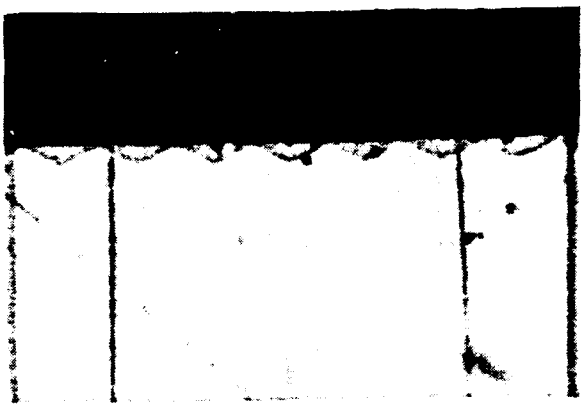

Fig. 2. End-view of periodic domains seen on y-face of lithium niobate wafer. Period of pattern is 10 μm, but sample is not the same as shown in Fig. 1.

used for birefringently phase-matched interactions, they are well-suited to quasi-phase-matched interactions using the d_{33} coefficient, which require only z-polarized modes. Initial experiments suggested that waveguides fabricated by the conventional exchange process in molten benzoic acid had an extremely small nonlinear susceptibility, so we instead used the annealed proton-exchange process from Ref. 26.

The first device that we constructed was a quasi-phase-matched frequency doubler for the 1.06 μm output of a CW Nd:YAG laser.[27] The device was fabricated on the $+z$ face of a 0.5 mm thick lithium niobate substrate obtained from Crystal Technology, Inc. For ease of fabrication, third-order QPM was used, so that the necessary grating period was approximately 18 μm. As the dispersion of the annealed proton-exchanged waveguides is not well-characterized, we fabricated the device with four 1 mm long Ti gratings with periods ranging from 15 to 22 μm arranged so that the pump beam would traverse all four gratings. The Ti gratings consisted of a 50 Å thick film patterned with liftoff lithography into 4 μm wide bars. The heat treatment consisted of a 2 h ramp from room temperature to 1100°C, a 30 min soak at 1100°C, and cooling back to room temperature at an initial rate of 8 K/min. A planar waveguide was then fabricated with a 30 min soak at 200 °C in pure benzoic acid followed by annealing in flowing oxygen at 350°C for 4 h. The resulting waveguide supported one TM mode at 1.06 μm.

Rutile prisms were used for input and output coupling of radiation to characterize the device. The input radiation was focused in the plane of the waveguide with an 8-cm focal length cylindrical lens. A TM-polarized output of 0.5 nW at 532 nm was measured for 1 mW of TM-polarized CW 1.06 μm outcoupled power, yielding a normalized conversion efficiency of 5%/W-cm^2.

To estimate the theoretical conversion efficiency, we modeled the device as a step-index guide with a refractive index difference of 0.003 and an in-plane beam waist of 30 μm. For waveguide depths in the range 4 to 7 μm, the calculated efficiency is 7 to 10%/W-cm^2, in good agreement with the observed conversion efficiency, and approximately 1500 times larger than would have been obtained in the absence of phase-matching.

The next devices used a finer grating to shift the operating wavelength to the vicinity of 800 nm.[28] The poling process was similar to that for the green doubler, but gratings of 6.5, 7, 7.5, and 7.75 μm periods, with 2 μm wide Ti lines were used. The heat treatment, again carried out in a closed crucible filled with congruent lithium niobate powder, was scaled to shorter times because of the shorter grating period. A ramp from room temperature to 1100°C in 2 h was followed by a 10 minute soak at 1100°C and a ramp back to room temperature with an initial cooling rate of 8 K/min. Both planar and channel

waveguides were fabricated in these substrates. The channel waveguides were fabricated by proton exchange through 3 μm wide channels in a 2000 Å thick aluminum film deposited on the substrate. The exchange was in pure benzoic acid for 20 min at 200°C, after which the mask was removed in a solution of sodium hydroxide. The sample was then annealed for 3 h at 350°C in flowing oxygen. Fabrication of the planar waveguides was identical with the exception of the masking step. The end faces of the channel samples were polished to produce a finished device approximately 1 cm long.

Optical measurements of the planar waveguides, which supported one TM mode at 850 nm, were made with a CW Styryl-9 dye laser and prism coupling. The normalized conversion efficiency into the TM_0 mode at 424 nm was 2%/W-cm^2, 5 to 10 times lower than theoretical estimates.

The channel devices were characterized with dye-laser radiation launched through a microscope objective in an end-fire geometry. With an 820-nm pump, the $1/e^2$ in-plane diameter of the fundamental and second harmonic modes were approximately 3.7 and 2.1 μm, respectively, and the out-of-plane diameters were 3.1 and 1.5 μm. The dependence of the output power on the pump wavelength is shown in Fig. 3, along with a sinc^2 curve fitted to the data. The FWHM of 0.5 nm is in reasonable agreement with the theoretical value of 0.4 nm obtained under the assumption that the dispersion of the proton-exchanged material is the same as that of congruent lithium niobate.[29] A plot of the TM polarized output power at 410 nm vs the square of the TM input power at 820 nm is shown in Fig. 4, illustrating the quadratic dependence up to 940 nW, the highest blue output power measured. The internal normalized conversion efficiency, corrected for 14% Fresnel reflection at the end face, is 37%/W-cm^2. The order of magnitude increase in efficiency over the planar device is expected from the in-plane mode confinement, but the conversion remains smaller than the theoretical value. The discrepancy for both the planar and the channel guides is probably due to the shallower domains that result from the short coherence length of this interaction, which reduce the overlap with the modal fields (Eq. 7).

The first step in improving these devices is to increase the length from 1 mm to 1 cm. Since the conversion efficiency scales with the square of the interaction length, one would expect 37%/W conversion in such a device, and thus approximately 1 mW of blue output for 50 mW of infrared input. If the aspect ratio of the domains can be increased through improved processing techniques, the better overlap with the modal fields would yield an order of magnitude increase in the normalized conversion efficiency, to 350%/W-cm^2. Another order of magnitude improvement would result from the use of first-order, rather than third-order, QPM. Such first-order devices would require further increases in the aspect ratio of the domains, or else more strongly guiding waveguides that confine the modes to the periodically-poled region near the surface of the device. Thus, it is interesting to investigate the tradeoff in proton-exchanged waveguides between high proton concentrations for tight confinement and low proton

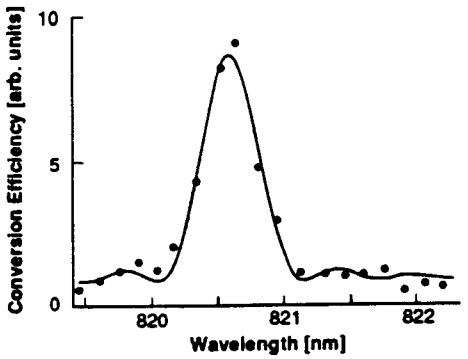

Fig. 3. Experimental wavelength tuning curve for second harmonic generation, shown with a fitted sinc^2 curve.

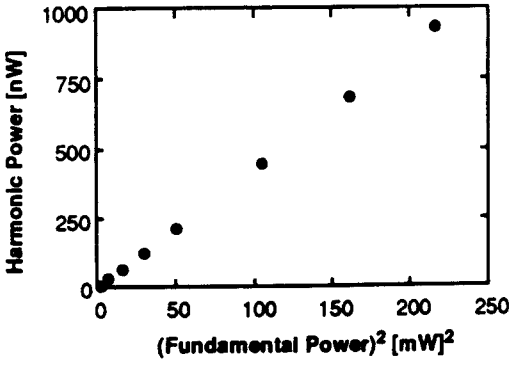

Fig. 4. Measured second harmonic power plotted against the square of the fundamental power, showing the quadratic relation between them.

concentrations to maintain the nonlinear susceptibility. Other topics currently under investigation include mixing two near-infrared sources in a periodically-poled channel waveguide to produce mid-infrared radiation, and the use of periodically-poled lithium tantalate waveguides for higher power applications where photorefractive damage may limit lithium niobate devices. The question of photorefractive damage in periodically-poled crystals is an open one, though indications exist that the magnitude of the effect is dramatically reduced, as is discussed in the following section.

4. LASER-HEATED PEDESTAL GROWTH OF PERIODICALLY-POLED CRYSTALS

An alternative approach to the production of periodically-poled lithium niobate is to grow crystals with reversed domains throughout their volume. Such crystals can be used in bulk optical devices, and would simplify the design of guided-wave devices by eliminating the penetration depth problem described in the previous section. This idea is not new; the effects of domain reversals on nonlinear optical interactions were investigated early in the history of nonlinear crystals.[30] Among the work that has been reported are techniques based on passing a pulsed current through the crystal either during[31] or after[32] growth, growth of a crystal rotated in an asymmetrical temperature field,[16] and growth at a periodically modulated rate.[31] The last of these techniques was employed during Stepanov growth, the remainder were applied to Czochralski grown crystals. However, widespread use of periodically-poled crystals has not yet been possible because of the difficulty in growing crystals meeting the strict periodicity criteria given in Eqs. (3) and (4). The best optical results were reported by Xue *et al.*[33], who demonstrated first order quasi-phase-matched SHG of a 1.06 μm pump in a crystal containing a 6.8-μm-period domain structure, approximately 100 periods of which contributed coherently to the interaction.

We report here on the growth of crystals up to 0.5 mm in diameter containing domain structures with periods as small as 2 μm, and on CW SHG of radiation with wavelengths as short as 407 nm.[34]

The crystals are grown in a laser-heated pedestal growth apparatus, described in Ref. 35, which uses the focused 10.6 μm output of a CO_2 laser to melt the tip of a typically 500-μm diameter source rod of either congruent composition or nominally 5% Mg-doped lithium niobate.[36] An oriented lithium niobate seed crystal is dipped into the melt, then withdrawn at a constant rate to pull the crystal while the molten zone is replenished by continuously feeding in the source rod. The ratio of the pull rate to the feed rate determines the diameter of the crystal. Crystals are grown either in air or a 4:1 mixture of helium and oxygen, at a typical rate of 2 mm/min. Lengths up to 5 cm of both *x*- and *z*-axis crystals are easily grown. The crystals are brownish after growth, but can be made transparent by annealing in dry flowing O_2 for several hours at 725°C.

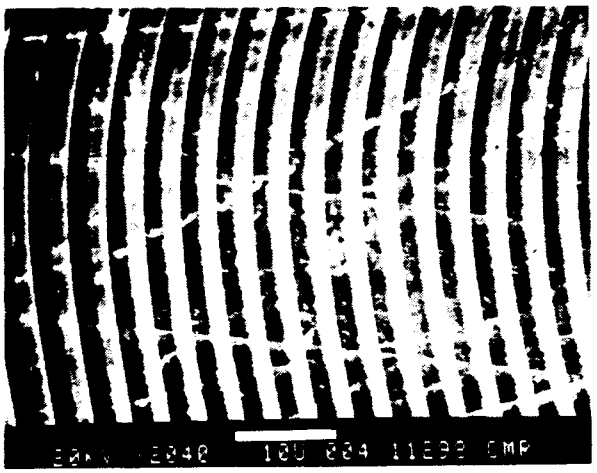

Fig. 5. SEM photograph of the *y* face of a polished and etched *x*-axis crystal, showing periodically-alternating domains with a period of approximately 3.5 μm. The curvature of the domains is due to the convex shape of the growth interface.

The domain structure of undoped crystals grown by this technique is discussed in Ref. 19; similar results have been obtained with Mg-doped crystals. *z*-axis crystals grow with a single domain, oriented with +*z* toward the melt, while *x*-axis crystals have a single domain wall perpendicular to the *z*-axis at the center of the crystal, dividing the crystal into two domains with the +*z*-axis pointing outward towards the surface. As discussed in Ref. 19, these patterns are most easily explained with the assumption that the domain orientation is controlled by thermoelectric fields generated by the large temperature gradients present in

this growth process, but composition gradients may also have an influence.

Periodically-poled crystals are grown by periodically perturbing the growth, either by rotating an asymmetric heat input created by a rotating mask in the CO_2 laser beam or by modulating the laser power. The period of the domain structures is given by $\Lambda = v_{pull} / f_{mod}$, where v_{pull} is the pull rate and f_{mod} is the frequency of the modulation. Using these techniques, it has been possible to produce domain structures with periods as small as 2 μm in both z- and x-axis crystals (Fig. 5). It is difficult to explain these results in terms of a model based on thermoelectric effects; it is probable that the domain reversals result from compositional striations induced by the periodic perturbation of the freezing interface. Models based on composition gradients have been advanced to explain the domain structures in bulk periodically-poled crystals.[37] While the microscopic mechanism responsible for the domain reversals remains a topic of current research, it appears that the large axial temperature gradients, high growth rates, and short dwell time at elevated temperatures characteristic of the laser-heated pedestal growth system aid in the formation of well-defined domain structures with small periods.

The sample used in the nonlinear optical experiments discussed here is a 1.77-mm long piece of a Mg-doped x-axis crystal approximately 250 μm in diameter, grown at a rate of 2 mm/min while the laser power was modulated at f_{mod} = 12.35 Hz. The resulting domain period, $\Lambda \approx 2.7$ μm, was chosen so that SHG using either the d_{33} or the d_{22} coefficient could be first-order quasi-phase-matched within the tuning range of a CW Styryl-9 dye laser. Figure 6 shows the phase-matching curves generated by tuning the wavelength of the dye laser, focused with a 5× microscope objective to a 6 μm diameter spot in the crystal. Curves (a) and (b) were obtained by polarizing the fundamental wave along the z and y axes, respectively. As expected, the polarization of the second harmonic was the same as that of the fundamental in both cases. The difference in the peak wavelengths, 814.5 nm for d_{33} and 850.5 for d_{22}, is due to the difference between the dispersion of n_e and and that of n_o.

The quality of the sample can be estimated from the effective interaction length, l_{eff}, inferred from the width of the tuning curves.[38] With the tight focus used to generate the curves in Fig. 6, l_{eff} is limited by the confocal length of the beam. To determine the limit on l_{eff} due to inhomogeneities in the crystal, the tuning curves were remeasured using a 65-mm focal-length lens to focus the beam, resulting in a confocal length of 1.3 mm. In this case the FWHM of the two curves were 1.4 nm and 1.5 nm for d_{33} and d_{22}, respectively. Using the dispersion data of Ref. 29, $l_{eff} \approx 320$ μm was obtained for both d_{33} and d_{22}, corresponding to an effective number of domains $N \approx 240$. That the same effective length was obtained for both polarizations suggests that it is limited by variations in the domain spacing rather than by compositional inhomogeneities, as the latter generally affects the two indices of refraction differently.

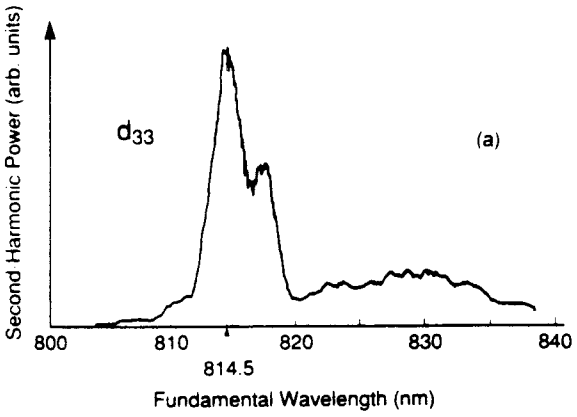

Fig.6(a). Second harmonic power vs fundamental wavelength, for extraordinary polarization, focusing with 5× objective.

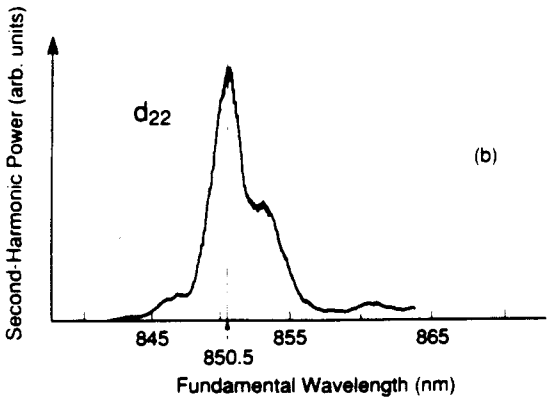

Fig. 6(b). Same as (a), except ordinary polarization.

According to Eq. (4), the accumulated error in the position of the Nth domain is approximately $\Lambda/2 \approx 1.3$ μm, a magnitude not unlikely given the slippage in the friction-coupled belt-drive system, designed to pull long continuous lengths of fiber for other applications, used to translate the lithium niobate fibers during growth.

The theoretical conversion efficiency was calculated using $d_{eff} = 22$ pm/V, obtained from Eq. (2) and the value for d_{33} from Ref. 7, and $l_{eff} = 320$ μm. The conversion efficiency for the measurement with the 65-mm lens agreed within 20% with this calculation. With the 5× objective, close to the optimum focusing for this effective length, as much as 7 μW of blue light was generated with 83 mW of input at the fundamental. The normalized theoretical conversion efficiency for an optimally-focused interaction using d_{33} and QPM is 5.2%/W-cm, 13.5 times larger than would be obtained for a birefringently phase-matched interaction using d_{31} (were it possible to phase-match).

Photorefractive damage is an important consideration for applications of lithium niobate involving visible radiation.[39] In lithium niobate, a bulk photovoltaic effect is responsible for the charge separation that leads to the changes in the index of refraction that cause the light scattering. The sign of this current changes in antiparallel domains, so one would expect the photorefractive effect to be substantially altered in periodically-poled crystals. To test this supposition, we compared the photorefractive response of an ≈ 2 mm long, undoped x-grown periodically-poled sample with $\Lambda = 3$ μm against that of an identically-prepared uniformly-poled sample. 488-nm radiation from an argon laser was polarized along the z-axis and focussed to a 12-μm diameter spot inside the sample. An adjustable slit, oriented so that photorefractive beam spreading along the z-axis would reduce the proportion of the beam transmitted, was centered in the far-field of the transmitted beam at a very low input power and adjusted to block approximately half the total power. The power was then increased, and the time-dependent throughput of the slit was recorded. The results depended on the power of the input beam; typically an initial rapid (100 ms – 10 s) decrease in throughput was followed by a slow recovery (10 s – 10 min) to a level somewhat below the original low-power value. For the uniformly poled sample with 100 mW incident power, the fraction passed by the slit dropped to less than 40% of the low power value in 100 ms. Under the same conditions, no significant reduction in the throughput was seen with the periodically-poled sample. As is typical of photorefractive phenomena, the behavior was a complicated function of input power, thermochemical history of the samples, etc., so more studies are necessary to properly characterize the effect. However, the present data support the hypothesis that the optically-induced changes in the index of refraction are dramatically altered by the domain reversal, and suggest that periodically-poled lithium niobate can support useful intensities of blue light at room temperature.

In future work, the crystals will be pulled with precision linear stages to improve the uniformity of the domain structures and thus increase the effective length of the crystal. Assuming losses comparable to bulk crystals, even the present periodically-poled crystals are adequate to produce milliwatts of blue power from commercially available diode lasers if used in resonantly-enhanced SHG devices.[1,2] Samples are currently being prepared for use in intracavity second harmonic generation in a 946-nm Nd:YAG laser. Further characterization and modeling of the photorefractive effect in perodically-poled crystals are also of interest.

5. CONCLUSIONS

Periodically-poled lithium niobate can be engineered to quasi-phase-match any nonlinear interaction within the transparency range of the the crystal at any desired temperature, using any nonlinear coefficient. Control over the phase-matching makes this readily-available crystal applicable to a broad range of interactions. We have produced periodically-poled lithium niobate both by processing the surface of uniformly-poled wafers and through the growth of crystals containing volume gratings of domains. Domain structures with periods as small as 5 μm in the planar material and 2 μm in the bulk material have been produced. Quasi-phase-matched SHG of CW blue and green radiation has been demonstrated in planar and channel annealed proton-exchange waveguides with a normalized efficiency of 37%/W-cm^2, as

has SHG of blue light in the bulk samples. Photorefractive damage resistance at room temperature is dramatically increased in the periodically-poled crystals. Improved single-pass waveguide devices and resonant bulk interactions both appear capable of generating milliwatts of blue light from available laser diodes. Infrared generation by mixing near-infrared diodes is also possible.

6. ACKNOWLEDGMENTS

We are grateful to Crystal Technology, Inc. for providing the substrates, and to T. Carver, L. Goddard, and J. Vrhel for assistance in fabrication. This work was supported by the Air Force Office of Scientific Research, contract AFOSR-88-0354, the Joint Services Electronics Program, contract N00014-84-K-0327, and IBM corporation, contract 703211.

7. REFERENCES

1. W. J. Kozlovsky, C. D. Nabors, and R. L. Byer, "Efficient Second Harmonic Generation of a Diode-Laser-Pumped CW Nd:YAG Laser Using Monolithic MgO:$LiNbO_3$ External Resonant Cavities," *IEEE J. Quantum Electron.* **24**, pp. 913–919 (1988).

2. G. J. Dixon, C. E. Tanner, and C. E. Wieman, "432-nm Source Based on Efficient Second-Harmonic Generation of GaAlAs Diode-Laser Radiation in a Self-Locking External Resonant Cavity," *Opt. Lett.* **14**, pp. 731–733.

3. G. I. Stegeman and C. T. Seaton, "Nonlinear Integrated Optics," *J. Appl. Phys.* **58**, pp. R57–R78 (1985).

4. G. Tohmon, K. Yamamoto, and T. Taniuchi, "Blue Light Source Using Guided Wave Frequency Doubler With a Diode Laser," *Proc. SPIE* **898**, pp. 70–75 (1988).

5. J. A. Armstrong, N. Bloembergen, J. Ducuing, and P. S. Pershan, "Interaction Between Lightwaves in a Nonlinear Dielectric," *Phys. Rev.* **127**, pp. 1918–1939 (1962).

6. K. C. Rustagi, S. C. Mehendale, and S. Meenakshi, "Optical Frequency Conversion in Quasi-Phase-Matched Stacks of Nonlinear Crystals," *IEEE J. Quantum Electron.*, **QE-18**, pp. 1029–1041 (1982).

7. S. K. Kurtz, J. Jerphagnon, and M. M. Choy, "Nonlinear Dielectric Susceptibilities," in *Landolt-Börnstein, New Series*, edited by K.-H. Hellwege (Springer-Verlag, Berlin, 1979), Vol. 11, p. 682.

8. M. M. Fejer, "Single Crystal Fibers: Growth Dynamics and Nonlinear Optical Applications," Ph.D. dissertation, Stanford University, Stanford, CA (1986).

9. A. Szilagyi, A. Hordvik, and H. Schlossberg, "A Quasi-Phase-Matching Technique for Efficient Optical Mixing and Frequency Doubling," *J. Appl Phys.* **47**, pp. 2025–2032 (1976).

10. D. E. Thompson , J. D. McMullen, and D. B. Anderson, "Second-Harmonic Generation in GaAs 'Stack of Plates' Using High-Power CO_2 Laser Radiation," *Appl. Phys. Lett.* **29**, pp. 113–115 (1976).

11. C. F. Dewey Jr. and L. O. Hocker, "Enhanced Nonlinear Optical Effects in Rotationally Twinned Crystals," *Appl. Phys. Lett.* **26**, 442–444 (1975).

12. G. Khanarian, D. Haas, R. Keosian, D. Karim, and P. Landi, "Phase Matched Second Harmonic Generation in a Polymeric Waveguide," paper ThB1, Conference on Lasers and Electro-Optics, Baltimore, MD, April 24-28, 1989.

13. R. C. Miller, "Optical Harmonic Generation in Single Crystal $BaTiO_3$," *Phys. Rev.* **134**, pp. A1313–A1319 (1964).

14. A. Räuber, "Chemistry and Physics of Lithium Niobate," in *Current Topics in Materials Science*, Vol. 1, edited by E. Kaldis (North-Holland, Amsterdam, 1978), pp. 481–601

15. A. Feisst and P. Koidl, "Current Induced Periodic Ferroelectric Domain Structures in $LiNbO_3$ Applied for Efficient Nonlinear Optical Frequency Mixing," *Appl. Phys. Lett.* **47**, pp. 1125–1127 (1985).

16. N. B. Ming, J. F. Hong, and D. Feng, "The Growth Striations and Ferroelectric Domain Structures in Czochralski-Grown $LiNbO_3$ Single Crystals," *J. Mater. Sci.* **17**, pp. 1663–1670 (1982).

17. K. Nakamura and H. Shimizu, "Poling of Ferroelectric Crystals by Using Interdigital Electrodes and its Application to Bulk-Wave Transducers," *1983 IEEE Ultrasonics Symp. Proc.*, pp. 527–530 (1983).

18. K. Nakamura, H. Ando, and H. Shimizu, "Ferroelectric Domain Inversion Caused in $LiNbO_3$ Plates by Heat Treatment," *Appl. Phys. Lett.* **50**, pp. 1413–1414 (1987).

19. Y. S. Luh, R. S. Feigelson, M. M. Fejer, and R. L. Byer, "Ferroelectric Domain Structures in $LiNbO_3$ Single-Crystal Fibers,"*J. Cryst. Growth* **78**, pp. 135–143 (1986).

20. J. R. Carruthers, G. E. Peterson, M. Grasso, and P. M. Bridenbaugh, "Nonstoichiometry and Crystal Growth of Lithium Niobate," *J. Appl. Phys.* **42**, 1846–1851 (1971).

21. E. J. Lim and M. M. Fejer, "Effects of Lithium Outdiffusion on Ferroelectric Domains in Lithium Niobate," in preparation for *Appl. Phys. Lett.*

22. J. Webjörn, F. Laurell, and G. Arvidsson, "Blue Light Generated by Frequency Doubling of Laser Diode Light in a Lithium Niobate Channel Waveguide," *IEEE Photonics Technology Letters* **1**, to be published October 1989.

23. S. Miyazawa, "Ferroelectric Domain Inversion in Ti-indiffused $LiNbO_3$ Optical Waveguide," *J. Appl. Phys.* **50**, pp. 4599–4603 (1979).

24. S. Thaniyavarn, T. Findakly, D. Booher, and J. Moen, "Domain Inversion Effects in Ti-$LiNbO_3$ Integrated Optic Devices," *Appl. Phys. Lett.* **46**, pp. 933–935 (1985).

25. S. K. Korotky and R. C. Alferness, "Ti:$LiNbO_3$ Integrated Optic Technology," in Integrated Optical Circuits and Components, Design and Applications, L. D. Hutcheson, ed., pp. 169–227, Marcel Dekker, Inc., New York, (1987).

26. P. G. Suchoski, T. K. Findakly, and F. J. Leonberger, "Stable low-loss proton-exchanged $LiNbO_3$ waveguide devices with no electro-optic degradation," *Opt. Lett.* **13**, pp. 1050–1052 (1988).

27. E. J. Lim, M. M. Fejer, and R. L. Byer, "Second Harmonic Generation of Green Light in Periodically Poled Planar Lithium Niobate Waveguide,"*Electron. Lett.* **25**, pp. 174–175 (1989).

28. E. J. Lim, M. M. Fejer, and R. L. Byer, "Blue Light Generation by Frequency Doubling in Periodically Poled Lithium Niobate Channel Waveguide," *Electron. Lett.* **25**, pp. 731–732 (1989).

29. G. J. Edwards and M. Lawrence, "A Temperature-Dependent Dispersion Equation for Congruently Grown Lithium Niobate," *Optical and Quantum Electronics* **16**, pp. 373–375 (1984).

30. R. C. Miller, "Optical Harmonic Generation in Single Crystal $BaTiO_3$," *Phys. Rev.* **134**, pp. A1313–A1319 (1964).

31. B. S. Red'kin, V. N. Kurlov, and V. A. Tatarchenko, "The Stepanov Growth of $LiNbO_3$ Crystals," *J. Cryst. Growth* **82**, pp. 106–109 (1987).

32. V. V. Antipov, A. A. Blistanov, N. G. Sorokin, and S. I. Chizhikov, "Formation of Regular Domain Structure in the Ferroelectrics $LiNbO_3$ and $LiTaO_3$ Near the Phase Transition," *Sov. Phys. Crystallogr.* **30**, pp. 428–430 (1985).

33. Y. H. Xue, N. B. Ming, J. S. Zhu, and D. Feng, "The Second Harmonic Generation in $LiNbO_3$ Crystals with Periodic Laminar Ferroelectric Domains," *Chinese Phys.* **4**, pp. 554–564 (1983).

34. G. A. Magel, M. M. Fejer, and R. L. Byer, "Quasi-Phase-Matched Second Harmonic Generation of Blue Light in Periodically-Poled $LiNbO_3$," submitted to *Appl. Phys. Lett.*

35. M. M. Fejer, J. L. Nightingale, G. A. Magel, and R. L. Byer, "Laser-Heated Miniature Pedestal Growth Apparatus for Single-Crystal Optical Fibers," *Rev. Sci. Instrum.* **55**, pp. 1791–1796 (1984).

36. The source rods for the congruent and the Mg-doped samples were cut from integrated optic substrates and nominally 5% Mg-doped $LiNbO_3$, respectively. Both were obtained from Crystal Technology, Inc., Palo Alto, CA.

37. J. Chen, Q. Zhou, J. F. Hong, W. S. Wang, N. B. Ming, D. Feng, and C. G. Fang, "Influence of Growth Striations on Para-Ferroelectric Phase Transitions: Mechanism of the Formation of Periodic Laminar Domains in $LiNbO_3$ and $LiTaO_3$," *J. Appl. Phys.* **66**, pp. 336–341 (1989).

38. S. Blit, E. G. Weaver, and F. K. Tittel, "Wavelength Temperature and Angle Bandwidths in SHG of Focused Beams in Nonlinear Crystals," *Appl. Opt.* **18**, pp. 733–736 (1979); F. R. Nash, G. D. Boyd, M. Sargent III, and P. M. Bridenbaugh, "Effect of Optical Inhomogeneities on Phase Matching in Nonlinear Crystals,"*J. Appl. Phys.* **41**, pp. 2564–2576 (1970). [These results had to be slightly modified for evaluating QPM spectral bandwidths.]

39. A. M. Glass, "The Photorefractive Effect," *Opt. Eng.* **17**, pp. 470–479 (1978).